Asymmetrical spiral spectra and orbital angular momentum density of non-uniformly polarized vortex beams in uniaxial crystals

Ling-Yun Shu(舒凌云), Ke Cheng(程科)†, Sai Liao(廖赛),
Meng-Ting Liang(梁梦婷), and Ceng-Hao Yang(杨嶒浩)

College of Optoelectronic Technology, Chengdu University of Information Technology, Chengdu 610225, *China*

(Received 17 March 2022; revised manuscript received 18 May 2022; accepted manuscript online 14 June 2022)

To explore the effect of non-uniform polarization on orbital angular momentum (OAM) in anisotropic medium, in this work investigated are the evolution of the spiral spectra and OAM densities of non-uniformly polarized vortex (NUPV) beams in uniaxial crystals propagating orthogonal to the optical axis, and also the case of uniformly polarized vortex (UPV) beams with left-handed elliptical polarization. In the input plane, the NUPV beams present their spiral spectra of m-mode concentrated at $m = l \pm 1$ modes rather than $m = l$ mode, and reveal the relation among topological charge l, mode of spiral spectra m and the power weight value R_m expressed by $l = \sum_{m=-\infty}^{\infty} mR_m$. The relation $l = \sum_{m=-\infty}^{\infty} mR_m$ is still satisfied for UPV beams in uniaxially anisotropic crystals, whereas for NUPV beams their relations are no longer valid owing to non-uniform polarization. Furthermore, the analysis indicates that the asymmetrical distribution of power weight of spiral spectra and the non-zero value in the sum of longitudinal OAM densities originate from the initial non-uniform polarization and anisotropy in uniaxial crystals rather than topological charges. In addition, the relation between spiral spectrum and longitudinal OAM density is numerically discussed. This work may provide an avenue for OAM-based communications, optical metrology, and imaging by varying the initial non-uniform polarization.

Keywords: non-uniformly polarized beams, spiral spectrum, spin angular momentum, orbital angular momentum, vortex

PACS: 42.55.–f, 42.81.Gs, 42.68.Ay, 42.50.Tx **DOI:** 10.1088/1674-1056/ac7860

1. Introduction

The influence of non-uniform polarization on angular momentums has inspired considerable enthusiasm in recent years.[1–5] Generally, angular momentum is comprised of orbital component related to helical wavefront of light beam and spin component associated with circular polarization.[6] The light beams with helical phases or vortex structures carry orbital angular momentum (OAM) per photon of $\pm l\hbar$ with topological charge l and reduced-Planck constant $\hbar$.[7,8] Circularly polarized beams originating from the helical trace of the vectorial optical field possess an intrinsic spin angular momentum (SAM) of $\pm\hbar$.[9,10] The spin–orbit interaction also plays an important role in producing novel optical phenomena such as microscopic, nano-optics, and surface plasmons fields.[11] The optical spin–orbit conversion can occur in the longitudinal component of the non-paraxial beam with non-uniform polarization.[12,13]

The decomposition of OAM or spiral spectrum is an important approach to dealing with OAM modes of complex optical fields. In isotropic media, a scalar beam presents symmetric power weight distribution of spiral spectra about a maximal weight $m = l$, and its longitudinal OAM density is also cylindrical symmetry or zero-value, and it is the sum of OAM density in the positive z direction and that in the negative z direction.[14,15] Asymmetric spiral spectra about the higher order Bessel–Gauss beams integrated in time (HOBBIT) system and the new Hermite–Gaussian (HG) vortex beam can be found in turbulence.[16,17] As typical anisotropic media, uniaxial crystals can show great flexibilities to design nonlinear optical elements.[18–20] It is natural to ask whether a vortex beam coupled with non-uniform polarization could show different properties of OAM in anisotropic media. Following our previous work,[21] we further explore the effect of non-uniform polarization on OAM (*i.e.*, spiral spectra and OAM densities) in uniaxially anisotropic crystals. The results obtained in our work reveal that an asymmetry in power weight of spiral spectra and the non-zero value in the sum of longitudinal OAM densities originate from the initial non-uniform polarization at the input plane and anisotropy in uniaxial crystals, and the multi-lobes of SAM can induce the non-zero value of OAM even in non-vortex. The conclusions are beneficial to the OAM-based communication, optical metrology, and imaging by varying the initial non-uniform polarizations and vortex cores.[22–24]

†Corresponding author. E-mail: ck@cuit.edu.cn

© 2023 Chinese Physical Society and IOP Publishing Ltd

2. Orbital angular momentum of NUPV beam in uniaxial crystal

Under the paraxial approximation, the x- and y-direction electric fields of the non-uniformly polarized vortex (NUPV) beams propagating in uniaxial crystals orthogonal to the optical axis in Cartesian coordinates obey the following equation:[25]

$$E_s(x,y,z) = \frac{kn_o e^{ikzn_q}}{2\pi iz}\iint_{\infty} dx_0 dy_0 E_s(x_0,y_0,0) \exp\left\{\frac{ik}{2zn_q}\left[n_o^2(x-x_0)^2+n_q^2(y-y_0)^2\right]\right\}, \quad (1)$$

where k is the wave number and the subscript $s = x$ or y, $q = e$ or $q = o$. If $s = x$, then $n_q = n_e$ (extraordinary refractive index), the sign $n_q = n_o$ (*i.e.*, ordinary refractive index) when $s = y$. The x and y components of the input electric field of $E_s(x,y,0)$ in Eq. (1) are expressed as[21,26,27]

$$\begin{pmatrix} E_x(x_0,y_0,0) \\ E_y(x_0,y_0,0) \end{pmatrix} = \begin{pmatrix} x_0\cos\theta - y_0\sin\theta \\ (y_0\cos\theta + x_0\sin\theta)\, e^{-i\delta} \end{pmatrix} \times (x_0 + i\,\mathrm{sgn}(l)\, y_0)^{|l|} \exp\left(-\frac{x_0^2+y_0^2}{w_0^2}\right), \quad (2)$$

where θ denotes the angle between polarization and radial direction, δ is the phase retardation angle between the x component and y component, $\mathrm{sgn}(l)$ is the sign function, w and l are the waist width and topological charge of vortex core, respectively. Under the condition of $\theta = 0$, $\delta = 0$ and $\theta = \pi/2$, $\delta = 0$, equation (2) reduces to the electric field of radially polarized vortex (RPV) beams and azimuthally polarized vortex (APV) beams, respectively. One can find that the NUPV beams can describe not only RPV and APV beams, but also a kind of hybridly polarized vortex (HPV) beams with linear, circular and elliptical polarization states in different spatial positions.

2.1. Spiral spectrum

To elucidate the spiral spectrum of the x- and y-direction electric field distributions, the complex field of $E_s(x,y,z)$ can be projected into spiral harmonics $e^{im\phi}$. The expanded expression in a cylindrical coordinate system is written as[28,29]

$$E_s(r,\phi,z) = \frac{1}{\sqrt{2\pi}}\sum_{m=-\infty}^{+\infty} a_m(r,z)\exp(im\phi), \quad (3)$$

where r and ϕ are radial coordinate and azimuthal coordinate with $x = r\cos\phi$ and $y = r\sin\phi$, and the expansion coefficient is expressed as

$$a_m(r,z) = \frac{1}{\sqrt{2\pi}}\int_0^{2\pi} E_s(r,\phi,z)\exp(-im\phi)\, d\phi. \quad (4)$$

The power weight of the spiral spectrum can be computed from

$$R_m = \frac{\int_0^{\infty}|a_m(r,z)|^2 r dr}{\sum_{m=-\infty}^{\infty}\int_0^{\infty}|a_m(r,z)|^2 r dr} = \frac{P_m}{\sum_{m=-\infty}^{\infty} P_m} \quad (5)$$

with the power of spiral spectrum P_m. Equation (5) provides a powerful way to explore the relative energy of each spiral spectrum of m-mode for the NUPV beams. Especially the spiral spectra of the input optical field with different polarization states are illustrated in Fig. 1. From Figs. 1(a1) and 1(a2), it is obvious that the spiral spectra of uniformly polarized vortex (UPV) beams centered at $m = l$ due to the embedded vortex cores with topological charge l, which indicates that these beams carry well-defined OAMs only at unique peak at $m = l$. However for NUPV beams their spiral spectra are concentrated at $m = l \pm 1$ modes as shown in Figs. 1(b1) and 1(d2), since the beam with non-vortex, *i.e.*, $l = 0$, incredibly carries the same spiral spectra at of $m = -1$ and $+1$ mode, respectively. One can find that the relation among topological charge l, mode of spiral spectra m and the power weight value R_m can be expressed as $l = \sum_{m=-\infty}^{\infty} mR_m$ in such symmetric OAM spectra.[30] For example, for the case of $l = 2$ in Figs. 1(b2)–1(d2), the power weights are 0.5 and 0.5 for $m = 1$ and 3, respectively, and their weight values are both equal to 0.5 for $m = -1$ and 1 with $l = 0$ as shown in Figs. 1(b1)–1(d1). These interesting phenomena demonstrate that spiral spectra of non-vortex optical fields can also be induced by non-uniform polarization in the initial field. The combined effect of non-uniform polarization and vortex structure leads to the concentration of spiral spectra at $m = l \pm 1$ modes.

Next, our attention is focused onto the evolution of spiral spectra of NUPV beams and UPV beams in uniaxial crystals. When the beams travel through a uniaxial crystal along the direction orthogonal to the optical axis, the y-component optical field follows the standard Fresnel diffraction in an isotropic medium with ordinary refractive index, the calculation results show that the weight values of spiral spectra of y-direction optical field always remain the same value of $R_{m=l\pm1} = 0.5$ in uniaxial crystal. Whereas the x-component optical field exhibits anisotropic diffraction, the evolution of spiral spectrum in an anisotropic medium is worth further studying. Unless otherwise specified, the abbreviation NUPV beam in the following refers to the x component of the case of $\theta = \pi/4$ and $\delta = 7\pi/8$ in Eq. (1), and its polarization is a hybrid morphology with linear, right-handed and left-handed elliptical polarizations. Besides, the abbreviation UPV beam refers to the x component of a uniformly polarized vortex beam with phase

retardation of $\delta = 3\pi/8$ in the following studies. The parameters are chosen to be $\lambda = 632.8$ nm, $w = 1$ mm, $n_o = 2.616$ (rutile crystals), and Rayleigh length $z_e = kw^2/2$.

Figures 2(a1)–2(a4) and 2(b1)–2(b4) show the evolutions of spiral spectra of NUPV and UPV beams in uniaxial crystals for different topological charge l at $n_e/n_o = 1.5$, respectively, and the weight curves of different spiral spectra in $l = 1$ and $l = -2$ are also described in Figs. 2(c1)–2(c4). One can find that spiral spectra concentrated at $m = l \pm 1$ modes spread to other modes along with the positive and negative directions at an interval of $\Delta m = 2$, which means that the power carried by initial spiral spectrum gradually disperses into those of other spiral spectra. In particular, the UPV beams still keeps symmetrical spiral spectra about a maximum weight value in uniaxial crystal, whereas for NUPV beams their distributions in spiral spectrum is asymmetrical. For example, the weight values of $m = -2$, 0, 2, 4 modes in NUPV beams as shown in $l = 1$ of Fig. 2(a2) are 0.018, 0.57, 0.39, 0.025 respectively, while their weight values of $m = -1$, 1, 3 in UPV beam (see $l = 1$ of Fig. 2(b2)) equal 0.034, 0.93, 0.034, respectively. The UPV beams also exhibit another type of symmetry, which does not exist in NUPV beams. When $|l|$ is the same, the weight value of the center position is the same, and the weight values on both sides of the center position are also symmetrically equal. Particularly in the case of NUPV beam as shown in weight curves in Figs. 2(c1) and 2(c2), the two initial weights of 0.5 centered at $m = l \pm 1$ modes present asynchronous behaviors. The weight of one mode starts to increase to a maximum value then it gradually decreases, but the other mode decreases to a lower weight. For the UPV beam the initial weight of $R_m = 1$ decreases monotonically to a stable value, and the synchronous increase of the weights at $m = -1$ and 3, or $m = -3$ and 5 can be found at $l = 1$ of Fig. 2(c3). A similar case can be also found at $l = -2$ of UPV beam in Fig. 2(c4). One can find that the equation of $l = \sum_{m=-\infty}^{\infty} mR_m$ still holds true when the UPV beam propagates in a uniaxial anisotropic crystal, but for the NUPV beam the equation no longer holds true because of the embedded non-uniform polarization. More detailed data of the relationship $l = \sum_{m=-\infty}^{\infty} mR_m$ are given in Appendix A. It means that non-uniform polarization in the initial optical field can lead to the asymmetrical distribution of spiral spectrum propagating in uniaxial crystals, which provides a potential method for modulating the power carried by OAM modes. The asymmetric distribution results from joint action of the non-uniform polarization of the input plane and the anisotropy of the uniaxial crystal. The topological charge only affects the position and weight value of spiral mode.

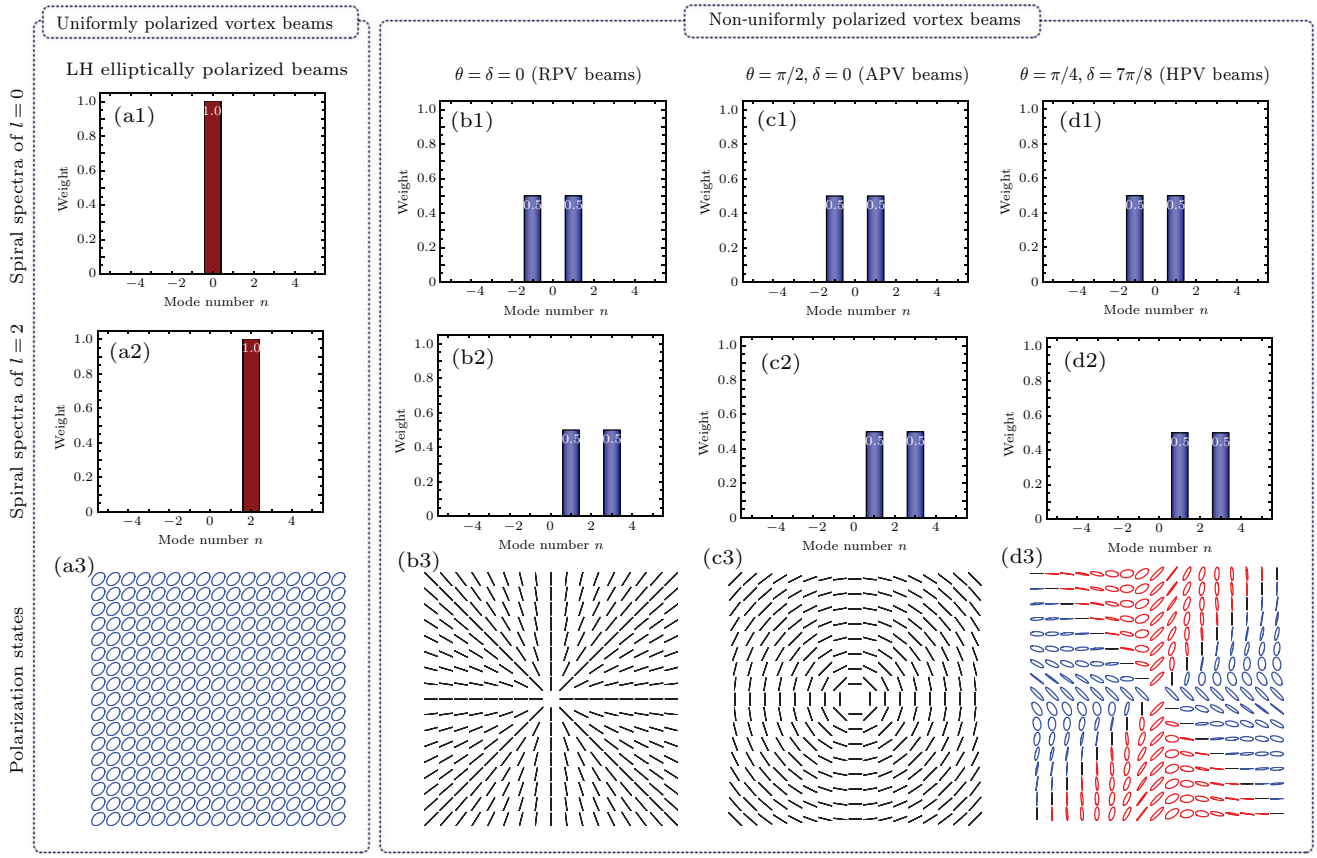


Fig. 1. Spiral spectra of input optical field with different polarization states. Top row: spiral spectra of $l = 0$; middle row: spiral spectra of $l = 2$; bottom row: the right-handed polarization (red), left-handed elliptical polarization (blue), and linear polarization (black). (a1)–(a3) uniformly polarized vortex beams; (b1)–(b3) radially polarized vortex beams; (c1)–(c3) azimuthally polarized vortex beams; (d1)–(d3) hybridly polarized vortex beams.

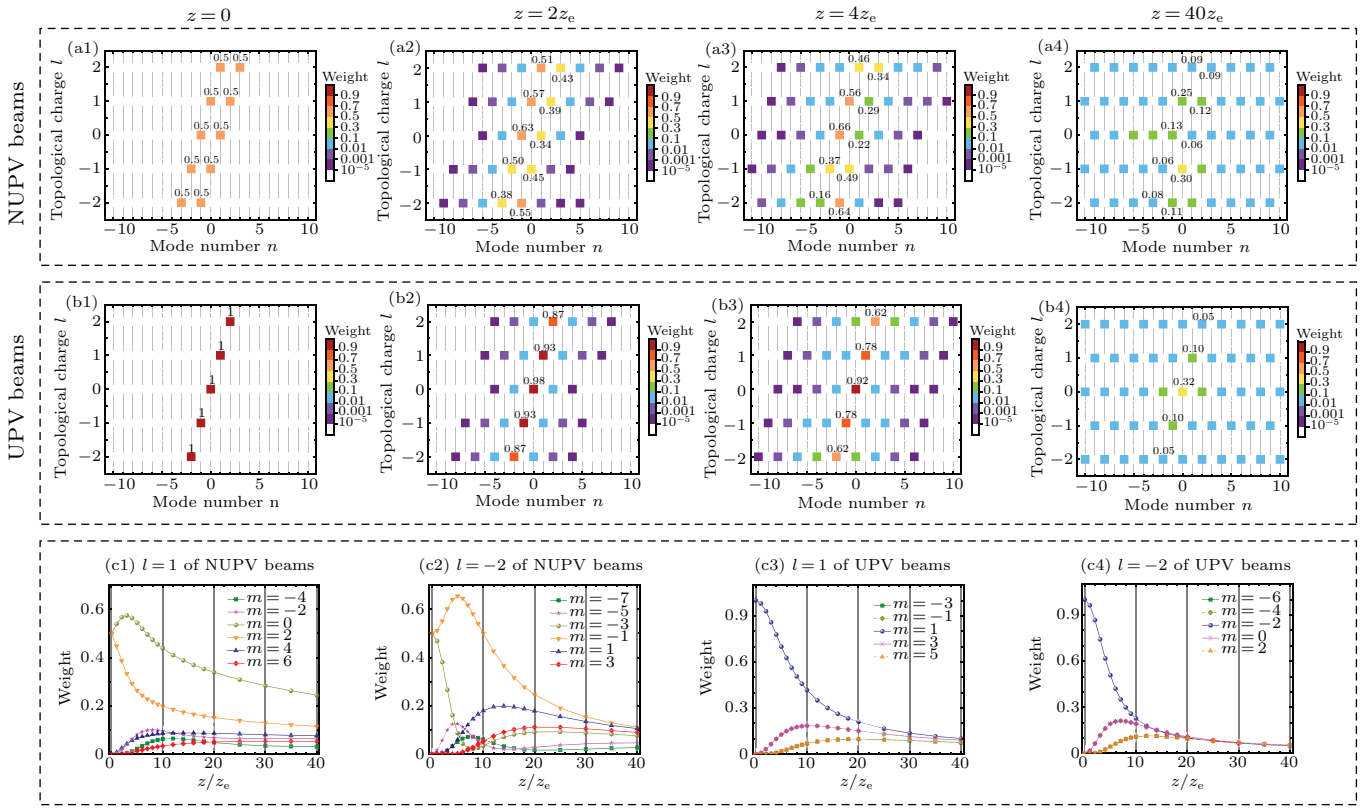


Fig. 2. Evolutions of spiral spectra and weight values of NUPV and UPV beams in uniaxial crystals for different values of l with $n_e/n_o = 1.5$. (a1)–(a4) NUPV beams; (b1)–(b4) UPV beams; (c1)–(c2) weight curves of spiral spectra of NUPV beams with $l = 1$ and $l = -2$; (c3)–(c4) weight curves of spiral spectra of UPV beams with $l = 1$ and $l = -2$.

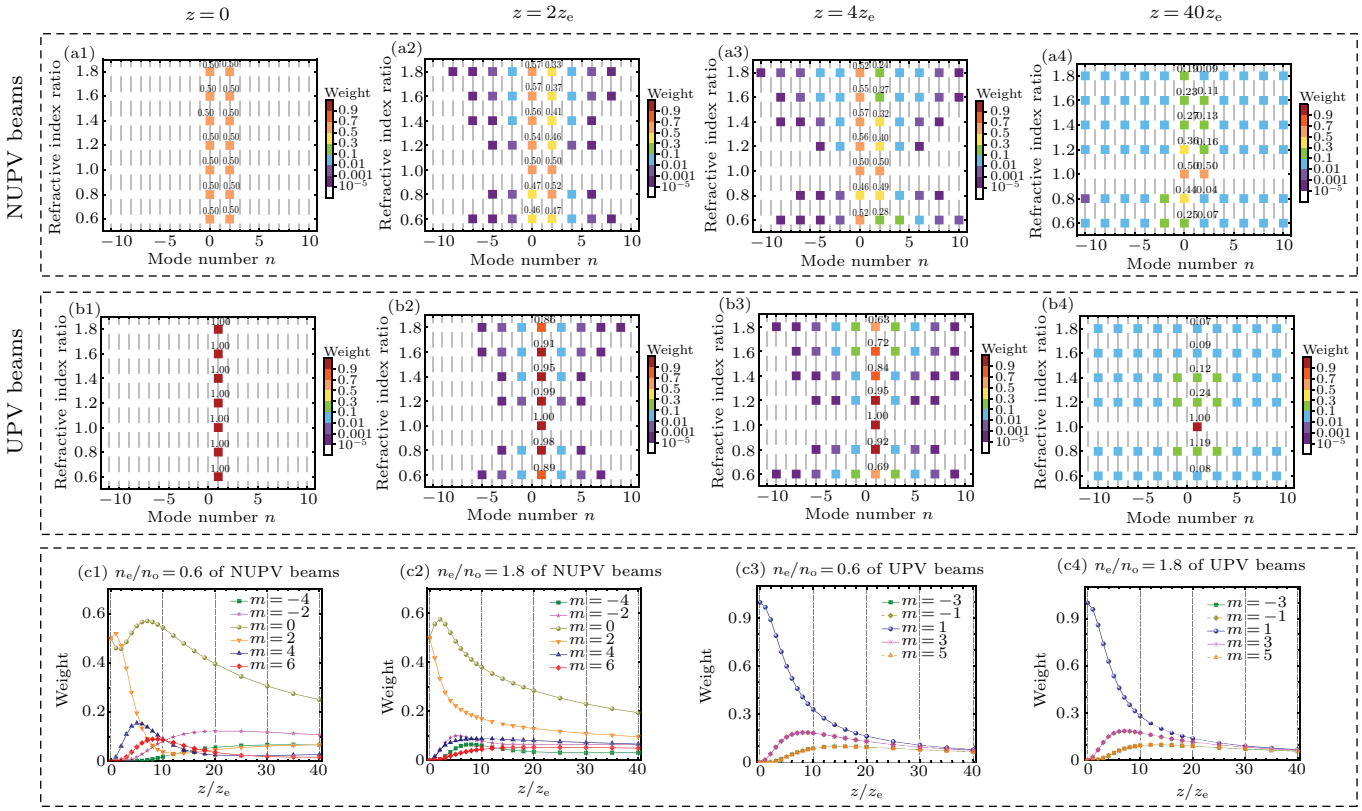


Fig. 3. Evolutions of spiral spectra and weight values of NUPV and UPV beams in uniaxial crystals for different values of refractive index ratio n_e/n_o with $l = 1$. (a1)–(a4) NUPV beams; (b1)–(b4) UPV beams; (c1)–(c2) weight curves of spiral spectra of NUPV beams with $n_e/n_o = 0.6$ and $n_e/n_o = 1.8$; (c3)–(c4) weight curves of spiral spectra of UPV beams with $n_e/n_o = 0.6$ and $n_e/n_o = 1.8$.

The effect of refractive index ratio n_e/n_o on spiral spectra of NUPV and UPV with $l = 1$ beams in uniaxial crystals are plotted in Figs. 3(a1)–3(a4) and 3(b1)–3(b4), respectively, and their weight curves in different modes at $n_e/n_o = 0.6$ and $n_e/n_o = 1.8$ are also given in Figs. 3(c1)–3(c4). It is clearly seen that the weights of spiral spectra always remain the same for $n_e/n_o = 1$, but the power at original modes can extend to other modes in anisotropic media for $n_e/n_o \neq 1$. More importantly, the extensions in weights of spiral spectra of UPV beams remain symmetrical in uniaxially anisotropic crystals for different values of n_e/n_o, but the distributions of weight value at spiral spectra are asymmetrical for NUPV beams. In addition, the weight values at $m = l = 1$ for UPV beams decrease monotonically, and the weights of other modes grow symmetrically with the increase of propagation distance z/z_e as shown in $n_e/n_o = 0.6$ and $n_e/n_o = 1.8$ of Figs. 3(c3)–3(c4). However for the NUPV beams the non-monotonic changes of weight at original modes $m = l \pm 1$, *e.g.*, $m = 0$ and $m = 2$ in Figs. 3(c1)–3(c2), also further verify the asymmetrical distributions of spiral spectra propagating in uniaxial crystals. The phenomenon means that the central mode with maximal weight in the NUPV beams can propagate in a lossless or high-quality behavior, and the energy loss even in the far field is much smaller than that of the UPV beams. These results indicate that the asymmetrical spiral spectra in propagation originate from the joint action of input non-uniform polarization states at the initial plane and the anisotropy in uniaxial crystals. For the input field of the NUPV beams, even in the absence of vortex embedding, there are still weights on non-zero modes. The central modes of the NUPV beams have larger weight values than those of the UPV beams. Therefore, the information carried in the NUPV beams will be lost less than that in the UPV beams, which implies that the NUPV beams in OAM-based communication have higher degrees of freedom,capacities and robustness than UPV beams.

2.2. Vectorial orbital angular momentum density

It is well established that the light beams with helical wave-front structures can carry OAM of $\pm l\hbar$ per photon.[31] The OAM in vectorial structures satisfies the following relationship:

$$\boldsymbol{L} = L_x \boldsymbol{e}_x + L_y \boldsymbol{e}_y + L_z \boldsymbol{e}_z, \tag{6}$$

where $\boldsymbol{e}_x$, $\boldsymbol{e}_y$, and $\boldsymbol{e}_z$ are the unit vectors along the positive x, y, and z axes, respectively. The components of L_x, L_y, and L_z are given by[32,33]

$$L_x \propto \mathrm{Im}\left(\sum_{j=x,y,z} E_j^* \left(y\frac{\partial E_j}{\partial z} - z\frac{\partial E_j}{\partial y}\right)\right), \tag{7}$$

$$L_y \propto \mathrm{Im}\left(\sum_{j=x,y,z} E_j^* \left(z\frac{\partial E_j}{\partial x} - x\frac{\partial E_j}{\partial z}\right)\right), \tag{8}$$

$$L_z \propto \mathrm{Im}\left(\sum_{j=x,y,z} E_j^* \left(x\frac{\partial E_j}{\partial y} - y\frac{\partial E_j}{\partial x}\right)\right). \tag{9}$$

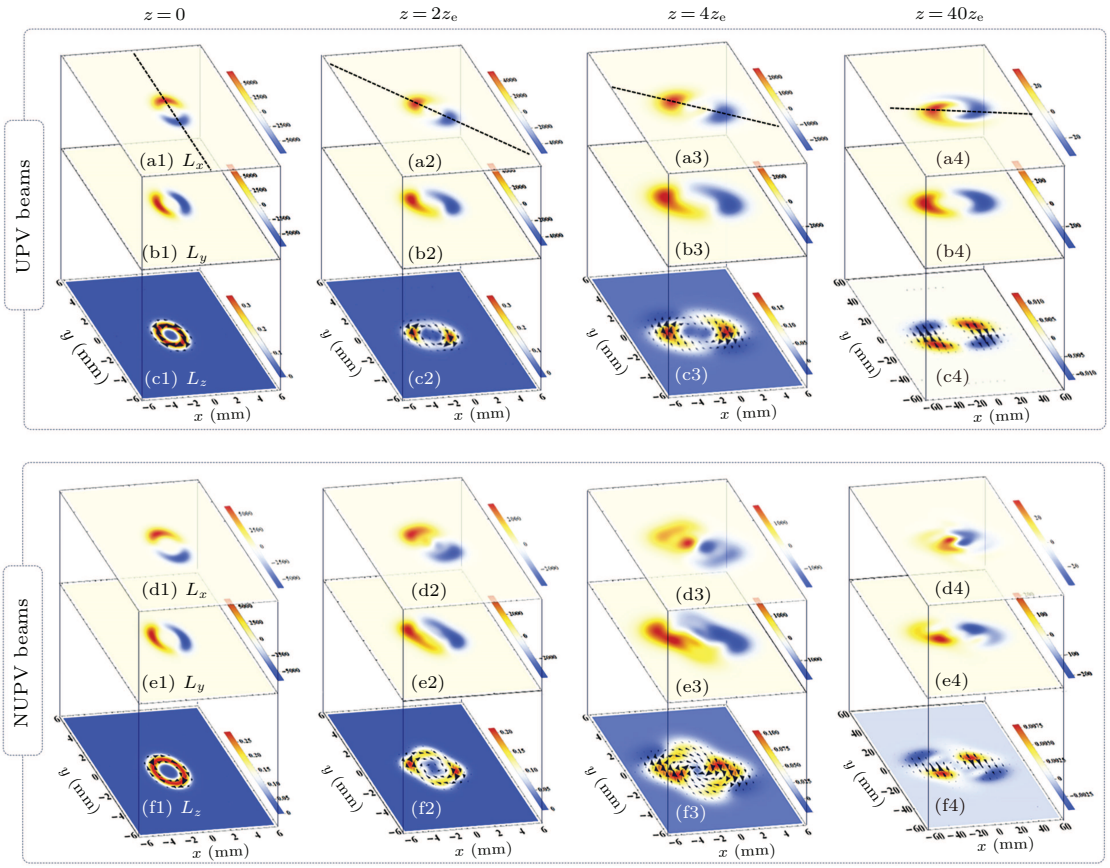


Fig. 4. The x , y, and z components of the OAM densities of NUPV and UPV beams in uniaxial crystals with topological charge $l = 2$ and $n_e/n_o = 1.5$, where the transverse OAM densities, *i.e.*, L_x and L_y, are also described by arrows. (a) and (d) L_x; (b) and (e) L_y; (c) and (f) L_z.

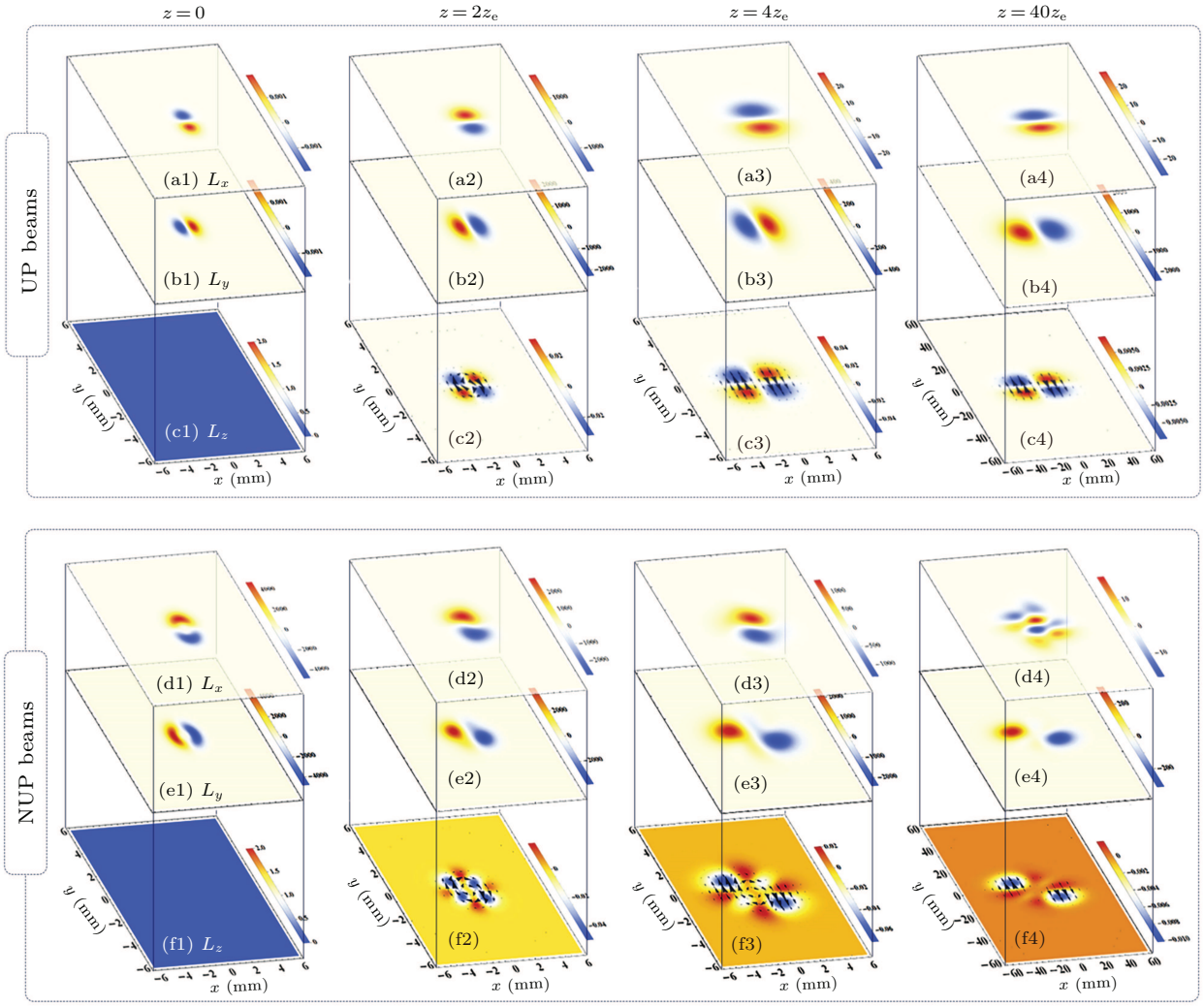


Fig. 5. The x , y, and z components of the OAM densities of non-uniformly polarized (NUP) beams and UP beams with non-vortex in uniaxial crystals, where the transverse OAM densities, *i.e.*, L_x and L_y, are also described by arrows. The parameters are $l=0$ and $n_e/n_o=1.5$. (a) and (d) L_x; (b) and (e) L_y; (c) and (f) L_z.

In an arbitrary polarization, the L_z component of light beam with non-vortex is generally equal to zero in free space or isotropic medium.[34] But the above analysis indicates that in uniaxially anisotropic crystals the spiral spectra of NUPV beams are asymmetrical due to non-uniform polarization at the input plane, our attention is paid to the effect of the embedded non-uniform polarization on the transversal and longitudinal OAM densities for non-vortex and vortex cases, respectively.

Numerical calculations taken from Eqs. (7)–(9) and shown in Figs. 4 and 5 are used to explore the evolution of OAM in vectorial structures in a uniaxial crystal. It is clearly seen that the longitudinal OAM densities of the NUPV beams with topological charge $l=2$ become distorted from circular structures at $z=0$ to non-cylindrical patterns at $z=40z_e$ in uniaxially anisotropic crystals as shown in Figs. 4(f1)–4(f4). For the transversal OAM densities, the uniformity of the pattern is destroyed as the transmission distance increases. The x-components of OAM densities, *i.e.*, L_x, display the rotation of two main-lobes anticlockwise. This can be seen intuitively from the rotation of the lobes in the transversal OAM density shown in Fig. 4, where the center positions of two main-lobes are connected by a dashed lines. One can see that dashed lines are rotated by two lobes anticlockwise. However, such an obvious rotation phenomenon is not found in L_y. Undoubtedly, the anisotropies in uniaxial crystals can lead to the distortion in OAM densities of NUPV and UPV beams due to faster spreading of light beams in the x direction for $n_e/n_o>1$, and the sum of L_z of NUPV beams and the sum of L_z of UPV beams, in the presence of vortex and polarization, are both not equal to zero. However, from Figs. 3(c4) and 3(f4), the sum of L_z of the UPV beams at the far field is closer to zero than that of the NUPV beams. What will happen if the vortex does not exist? For the case of $l=0$, the OAM densities of both beams in the input plane satisfy $L_z=0$ rather than circular structures as shown in Figs. 5(c1) and 5(f1). From Figs. 5(c1)–5(c4), one can find that the sum of L_z equals zero, with four stable lobes in longitudinal OAM densities for $l=0$. However, for non-uniformly polarized beams with non-vortex, the sum of the longitudinal OAM density, *i.e.*, L_z, is not equal to zero. These phenomena indicate that the non-zero appearance of the sums of L_z in

the NUPV beam is caused by a joint effect of the input non-uniform polarization and anisotropy.

Figure 6 further gives the z components of SAM and OAM densities of uniformly polarized (UP) and NUP beams with non-vortex in uniaxial crystals. Their OAM densities can be found for UP and NUP beams as shown in Figs. 6(b2) and 6(d2). The fact of $L_z = 0$ for UP beams even in anisotropic media indicates that the anisotropy in uniaxial crystal cannot change orbital angular momentum. Whereas for NUP beams the $L_z \neq 0$ in anisotropic medium means that the input non-uniform polarization, or the input multi-lobes SAM in Fig. 6(c1) can induce non-zero value in L_z. Therefore, the non-zero value in L_z is not caused by anisotropy, but by the input non-uniform polarization or the input multi-lobe SAM.

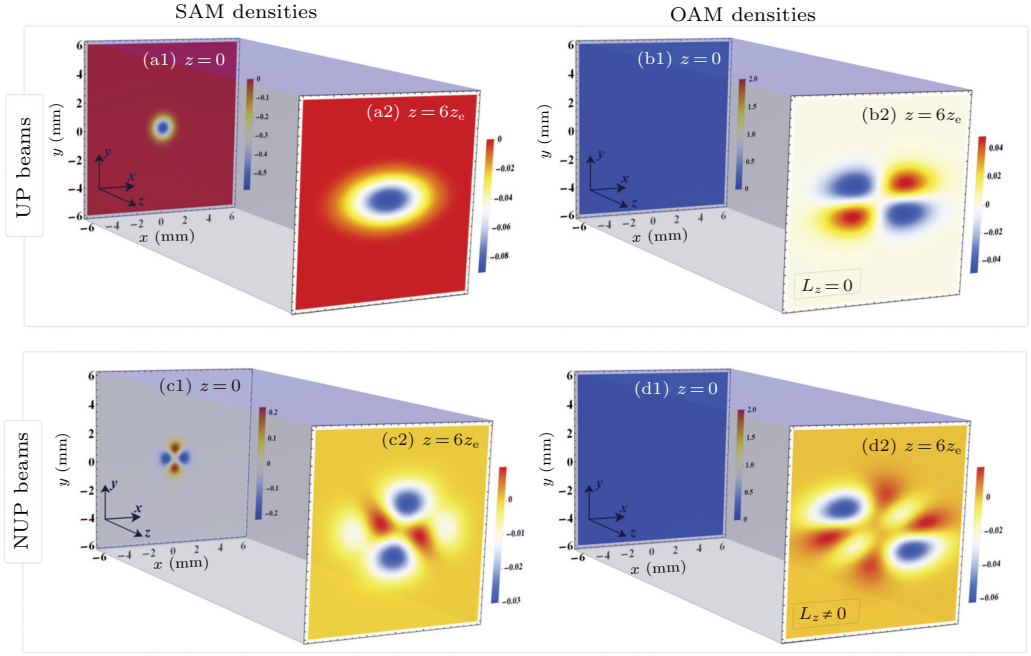


Fig. 6. The z components of SAM and OAM densities of UP and NUP beams with non-vortex in uniaxial crystals at different propagation distances. The parameters are $l = 0$ and $n_e/n_o = 1.5$. (a) and (c) SAM densities; (b) and (d) OAM densities.

2.3. Relation between spiral spectrum and longitudinal OAM density

The above analysis indicates that a non-uniform polarization can result in the asymmetrical distributions of spiral spectra and a non-zero value in the sum of L_z. The spiral spectra and longitudinal OAM densities provide different perspectives for exploring the evolution of OAM, and their relations are determined by[28,35]

$$L_z \propto \sum_{m=-\infty}^{\infty} mP_m. \tag{10}$$

To intuitively and numerically elucidate their relations, we define the ratio of positive part or negative part to the total OAM as

$$R_\sigma^{\pm} = \left|U_\sigma^{\pm}\right| / \left(\left|U_\sigma^{+}\right| + \left|U_\sigma^{-}\right|\right), \quad (\sigma = s \text{ or } d). \tag{11}$$

For spiral spectra, $R_s^{\pm}$ are the percentage of positive weight value and negative weight value, with $|U_s^{+}| = \sum_{m=1}^{\infty} mP_m$ and $|U_s^{-}| = \sum_{m=-\infty}^{-1} mP_m$, respectively.

For the longitudinal OAM densities, $R_d^{\pm}$ represent the percentage of positive total magnitude and the percentage of negative total magnitude, with $\left|U_d^{+}\right|$ and $\left|U_d^{-}\right|$ integrated by the longitudinal OAM densities.

Figure 7 displays the ratio of positive part and negative part to the total OAM of NUPV and UPV beams in uniaxial crystals for different values of refractive index ratio $n_e/n_o = 0.6$, 1, 1.8, and $l = 1$, respectively. From Figs. 7(a1) and 7(b1), it can be found that the values of R_σ^- in spiral spectra and longitudinal OAM densities both monotonically increase, and the values of R_σ^+ decrease in two different ways as shown in Figs. 7(a2) and 7(b2). When the NUPV beams propagate in uniaxial crystals, the increase the values of R_σ^- means that the weight of negative OAM gradually grows from zero-value, while the values of the positive part, *i.e.*, R_σ^+, decrease from maximal values. Compared with UPV beams, the NUPV beams present a greater range of change in R_σ^+ and R_σ^-. The results confirm that the asymmetrical distribution of spiral spectra as shown in Figs. 3(a1)–3(a4) in NUPV beams. The change of R_σ^+ and R_σ^- become increasingly intense with the augment of the difference between refractive index ratio n_e/n_o and 1, while for $n_e/n_o = 1$ the values of R_σ^+ and R_σ^- remain unchanged, which indicates that the anisotropy can further strengthen the asymmetrical distribution of spiral spectra and a non-zero value in the sum of L_z induced by non-uniform polarization.

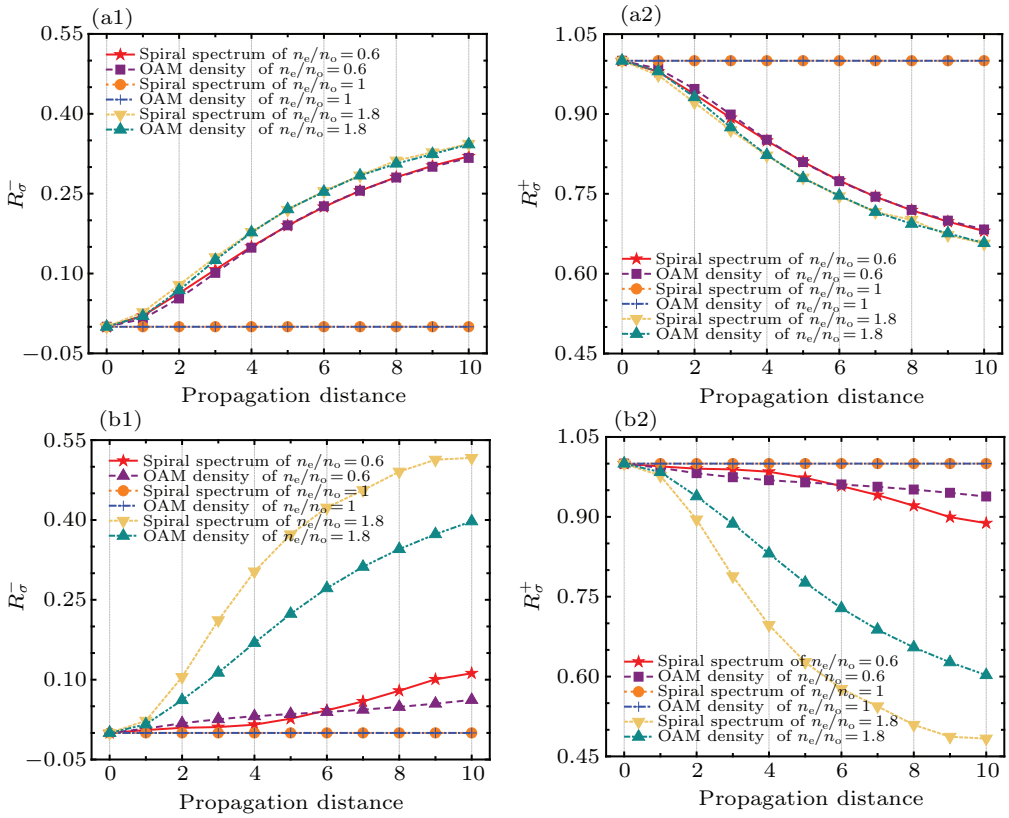


Fig. 7. Ratios of positive part R_σ^+ and negative part R_σ^- to the total OAM of NUPV and UPV beams in uniaxial crystals for different refractive index ratios $n_e/n_o = 0.6$, 1, 1.8, and $l = 1$, respectively. (a1) and (a2) UPV beams; (b1) and (b2) NUPV beams.

3. Conclusions

Based on the beam model in our previous work, the spiral spectra and OAM densities of NUPV and UPV beams in uniaxial crystals are further studied. For the NUPV beams, their positions of modes m concentrated at $m = l \pm 1$ rather than $m = l$ in spiral spectra, and the relation among topological charge l, mode of spiral spectra m and the power weight value R_m can be expressed as $l = \sum_{m=-\infty}^{\infty} mR_m$ at the input plane. In the uniaxially anisotropic crystals the relation of $l = \sum_{m=-\infty}^{\infty} mR_m$ still holds true for UPV beams, whereas for NUPV beams their relations are no longer valid due to the non-uniform polarization.

The influence of non-uniform polarization, topological charge and refractive index ratio on spiral spectra and OAM densities of NUPV and UPV beams are also explored by anisotropic diffraction in the x-component electric field. The UPV beams possess symmetrical power weights of spiral spectra even in anisotropic media, whereas the symmetrical distribution in power weights of spiral spectra disappears for the NUPV beams. The results show that the asymmetrical spiral spectra originate from the joint action of the input non-uniform polarization and anisotropy in uniaxial crystals. The topological charge affects the position and weight value of modes. Furthermore, the sum of the longitudinal OAM densities L_z for NUPV beams with non-vortex is not equal to zero, which are different from that of the UPV beams. It indicates that the non-zero value in L_z is related to the anisotropy and the input non-uniform polarization. The anisotropy in uniaxial crystals results in the extension of the spiral spectrum and the distortion of L_z. Based on such effects, the asymmetric spiral spectra and the non-zero values of the sums of L_z are obtained under the joint effect of anisotropy and input non-uniform polarization. These interesting phenomena may be explained by the conversion of optical SAM related to non-uniform polarization into OAM.[36] The relation between spiral spectrum and longitudinal OAM density is also discussed. The consistency of two different methods, *i.e.*, spiral spectra and OAM densities, in exploring OAM are numerically elucidated by the defined $R_\sigma^\pm$. The NUPV beams present a greater range of change in $R_\sigma^\pm$ than the UPV beams. The OAM change induced by the initial non-uniform polarization has potential applications in OAM-based communications, optical metrology and imaging.

Appendix A: Sums of mR_m of NUPV and UPV beams

To intuitively and accurately draw the conclusion about relation $l = \sum_{m=-\infty}^{\infty} mR_m$, Appendix A gives the sums of mR_m of NUPV and UPV beams during propagation in Fig. A1.

It can be obtained that regardless of the value of l, the sum of UPV beams still satisfies the relation $l = \sum_{m=-\infty}^{\infty} mR_m$ when propagating in a uniaxial crystal. For NUPV beams, the value of the sum decreases as the propagation distance increases and

the relation $l = \sum_{m=-\infty}^{\infty} mR_m$ does not hold true.

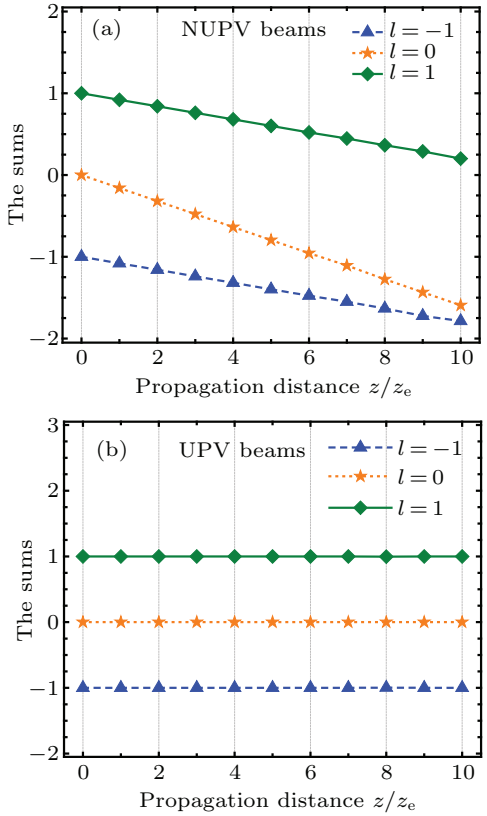


Fig. A1. Sums of mR_m of NUPV and UPV beams in uniaxial crystals with $n_e/n_o = 1.5$ and different values of vortex topological charge l. (a) NUPV beams; (b) UPV beams.

Acknowledgement

Project supported by the Science and Technology Program of Sichuan Province, China (Grant No. 23NSFSC1097).

References

[1] Pan Y, Gao X Z, Ma R D, Tu C H, Li Y N and Wang H T 2020 *Chin. Opt. Lett.* **18** 122601
[2] Alexeyev C N, Barshak E V, Lapin B P and Yavorsky M A 2018 *Phys. Rev. A* **98** 023824
[3] Han L, Qi S X, Liu S, Li P, Cheng H C and Zhao J L 2020 *Chin. Phys. B* **29** 094203
[4] Shi P, Du L P and Yuan X C 2018 *Opt. Express* **26** 23449
[5] Suzuki M, Yamane K, Oka K, Toda Y and Morita R 2016 *Phys. Rev. A* **94** 043851
[6] Shen Y J, Wang X J, Xie Z W, Min C J, Fu X, Liu Q, Gong M L and Yuan X C 2019 *Light: Sci. Appl.* **8** 90
[7] Yang Y J, Zhao Q, Liu L L, Rosales-Guzmán C and Qiu C W 2019 *Phys. Rev. Appl.* **12** 064007
[8] Zhao Q, Dong M, Bai Y H and Yang Y J 2020 *Photon. Res.* **8** 745
[9] O'Neil A T, MacVicar I, Allen L and Padgett M J 2002 *Phys. Rev. Lett.* **88** 053601
[10] Bai Y H, Lv H R, Fu X and Yang Y J 2022 *Chin. Opt. Lett.* **20** 012601
[11] Forbes K A and Andrews D L 2019 *Phys. Rev. A* **99** 023837
[12] Bliokh K Y, Alonso M A, Ostrovskaya E A and Aiello A 2010 *Phys. Rev. A* **82** 063825
[13] Chen R P, Chew K H, Dai C Q and Zhou G Q 2017 *Phys. Rev. A* **96** 053862
[14] Sztul H I and Alfano R R 2008 *Opt. Express* **16** 9411
[15] Ji Z Y and Zhou G Q 2017 *Chin. Phys. B* **26** 094202
[16] Watkins R J, Dai K, White G, Li W, Miller J K, Morgan K S and Johnson E G 2020 *Opt. Express* **28** 924
[17] Li Y, Yu L and Zhang Y X 2017 *Opt. Express* **25** 12203
[18] Ciattoni A, Crosignani B and Porto P D 2001 *J. Opt. Soc. Am. A* **18** 1656
[19] Ciattoni A, Cincotti G, Provenziani D and Palma C 2002 *Phys. Rev. E* **66** 036614
[20] Liu D J, Wang H, Wang Y C and Yin H M 2015 *Opt. & Laser Tech.* **73** 12
[21] Shu L Y, Cheng K, Liao S, Liang M T and Zhu B Y 2021 *Optik* **243** 167464
[22] Willner A E, Huang H, Yan Y, Ren Y X, Ahmed N, Xie G D, Bao C J, Li L, Cao Y W, Zhao Z, Wang J, Lavery M P J, Tur M, Ramachandran S, Molisch A F, Ashrafi N and Ashrafi S 2015 *Adv. Opt. Photon.* **7** 66
[23] Kaushal H and Kaddoum G 2017 *IEEE Commun. Surv. Tutor.* **19** 57
[24] Sun Z C, Yan M Y and Xu B J 2020 *Chin. Phys. B* **29** 104101
[25] Ciattoni A and Palma C 2003 *J. Opt. Soc. Am. A* **20** 2163
[26] Xu K, Yang Y F, He Y, Han X H and Li C F 2010 *J. Opt. Soc. Am. A* **27** 572
[27] Cheng K, Jiao L Y and Zhong X Q 2016 *Opt. Commun.* **367** 112
[28] Torner L, Torres J P and Carrasco S 2005 *Opt. Express* **13** 873
[29] Liu Y D, Gao C Q, Qi X Q and Weber H 2008 *Opt. Express* **16** 7091
[30] Kotlyar V V and Kovalev A A 2021 *J. Opt. Soc. Am. A* **38** 1276
[31] Radwell N, Hawley R D, Götte J B and Franke-Arnold S 2016 *Nat. Commun.* **7** 10564
[32] Allen L, Beijersbergen M W, Spreeuw R J C and Woerdman J P 1992 *Phys. Rev. A* **45** 8185
[33] Enk S J V and Nienhuis G 1992 *Opt. Commun.* **94** 147
[34] Zhou G Q, Ji Z Y and Ru G Y 2016 *Laser Phys.* **26** 075002
[35] Cheng M J, Guo L X, Li J T, Huang Q Q, Cheng Q and Zhang D 2016 *Appl. Opt.* **55** 4642
[36] Kobayashi H, Nonaka K and Kitano M 2012 *Opt. Express* **20** 14064